Synthesis of $SnNb_2O_6$ Nanoplates and Their Photocatalytic Properties

Yasuhiro Hosogi,[1] Hideki Kato,[1] and Akihiko Kudo*[1,2]
[1]*Department of Applied Chemistry, Faculty of Science, Tokyo University of Science, 1-3 Kagurazaka, Shinjuku-ku, Tokyo 162-8601*
[2]*Core Research for Evolutional Science and Technology, Japan Science and Technology Agency (CREST, JST)*

(Received February 17, 2006; CL-060203; E-mail: a-kudo@rs.kagu.tus.ac.jp)

The visible light-driven photocatalyst $SnNb_2O_6$ was synthesized by reacting $Sr_2Nb_2O_7$ with molten $SnCl_2$ at 573 K. SEM observations revealed that the $SnNb_2O_6$ sample had a surface area of 56 $m^2 g^{-1}$, with particles having a nanoplate shape, a thickness of ca. 10 nm and widths of several hundred nm. A Pt-loaded $SnNb_2O_6$ nanoplate sample showed photocatalytic activity for H_2 evolution from an aqueous methanol solution under visible light irradiation.

Photocatalytic water splitting has attracted much interest. Many metal oxide photocatalysts that can split water into H_2 and O_2 in stoichiometric amounts with high efficiencies under ultraviolet light irradiation have been reported.[1–4] Moreover, many new photocatalysts that are active for H_2 or O_2 evolution from water containing sacrificial reagents under visible light irradiation have recently been found.[2] We have reported that $SnNb_2O_6$ is a rare oxide photocatalyst which is active for H_2 evolution from an aqueous methanol solution under visible light irradiation.[5] In $SnNb_2O_6$, the Sn 5 s orbital corresponding to Sn^{2+} contributes to the valence band formation, resulting in a narrow band gap. On the other hand, $KCa_2Nb_3O_{10}$ is a photocatalyst for water splitting under ultraviolet light irradiation when the exfoliated nanosheets are restacked, although the bulk $KCa_2Nb_3O_{10}$ does not decompose water.[6] In this case, the photocatalytic properties of $KCa_2Nb_3O_{10}$ are improved by the change in the morphology from bulk structure to lamellar aggregates. That result suggests that the characteristic nanosize morphology might be advantageous for photocatalytic performance. In the present study, $Sr_2Nb_2O_7$ with Sn(II) substituted for Sr, i.e., $Sr_{2-x}Sn_xNb_2O_7$, and $SnNb_2O_6$ with characteristic morphologies were synthesized from $Sr_2Nb_2O_7$, which has a layered perovskite structure, by molten $SnCl_2$-treatment. Their photocatalytic activities for H_2 evolution were examined.

$Sr_2Nb_2O_7$ powders were prepared by a flux method. Starting materials used were as follows: $SrCO_3$ (Kanto Chemical, purity; 99.9%), Nb_2O_5 (Kanto Chemical, purity; 99.95%), and H_3BO_3 (Kanto Chemical, purity; 99.5%). The molten $SnCl_2$-treatment was carried out by immersing $Sr_2Nb_2O_7$ in molten $SnCl_2$ (Wako, purity; 99.9%) at 573 K under flowing nitrogen. The samples treated with molten $SnCl_2$ for 15 min, 5 h, and 24 h were denoted as $Sr_2Nb_2O_7$(Sn-15 min), $Sr_2Nb_2O_7$(Sn-5 h), and $Sr_2Nb_2O_7$-(Sn-24 h), respectively. After the molten salt treatment, excess $SnCl_2$ was removed with HCl (1 mol L^{-1}). $SnNb_2O_6$, synthesized by solid-state reaction from SnO (Wako, purity; 99.9%) and Nb_2O_5, is denoted as $SnNb_2O_6$(SSR). The crystal structures of the synthesized oxides were confirmed by powder X-ray diffraction (Rigaku, MiniFlex). Diffuse reflectance spectra were measured using a UV–vis–NIR spectrometer with an integrating sphere (JASCO, Ubest-570). The surface area was determined by the BET method (Coulter, SA3100). The catalysts were observed with a scanning electron microscope (JEOL, JSM-6700F). The photocatalytic reactions of H_2 evolution from an aqueous methanol solution (10 vol %) and O_2 evolution from an aqueous silver nitrate solution (0.05 M) were conducted in a gas-tight circulation system. This reaction procedure basically followed an earlier report by the present authors.[5]

Figure 1 shows SEM photographs of $Sr_2Nb_2O_7$ and molten $SnCl_2$-treated $Sr_2Nb_2O_7$. The non-treated $Sr_2Nb_2O_7$ has a large plate-like particle with a width of 5 μm. The characteristic plate structure of the layered perovskite was broken up with increasing treatment time in molten $SnCl_2$. In contrast, $Sr_2Nb_2O_7$(Sn-24 h) is an aggregate of nanoplates with a ca. 10 nm thickness and widths of several hundred nanometers. EDS analysis revealed that the ratio of Sn to Sr increased with increasing treatment time in molten $SnCl_2$. After 15 min treatment, 20 mol % of the Sr in $Sr_2Nb_2O_7$ was substituted with Sn. After 24 h treatment, most Sr was substituted, yielding a 1:2 molar ratio of Sn to Nb.

Figure 2 shows XRD patterns of molten $SnCl_2$-treated $Sr_2Nb_2O_7$ and $SnNb_2O_6$(SSR). The $Sr_2Nb_2O_7$(Sn-15 min) sample (20 mol % Sn) maintained the layered perovskite structure. The particles obtained were a mixture of layered perovskite and $SnNb_2O_6$ when the treatment time in molten $SnCl_2$ was more than 15 min. $Sr_2Nb_2O_7$ was changed from $Sr_{2-x}Sn_xNb_2O_7$ to $SnNb_2O_6$ with an increase in the treatment time by molten $SnCl_2$. Aggregates of the nanoplates obtained by molten $SnCl_2$ treatment for 24 h were $SnNb_2O_6$ and a small amount of layered perovskite phase. The formation of $SnNb_2O_6$ was also confirmed by Raman measurements. The broad peaks of XRD pattern were due to the fine particle and low crystallinity of $SnNb_2O_6$ nanoplate. The surface area of the nanoplates was large (56 $m^2 g^{-1}$).

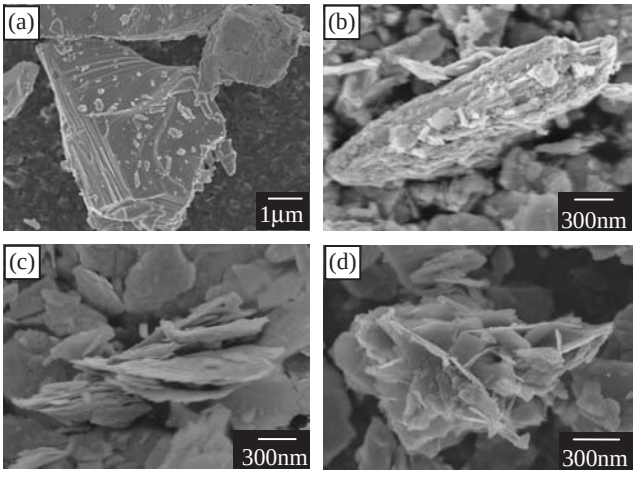

Figure 1. Scanning electron microscope images of molten $SnCl_2$-treated $Sr_2Nb_2O_7$. (a) Non-treated, (b) $Sr_2Nb_2O_7$(Sn-15 min), (c) $Sr_2Nb_2O_7$(Sn-5 h), and (d) $Sr_2Nb_2O_7$(Sn-24 h).

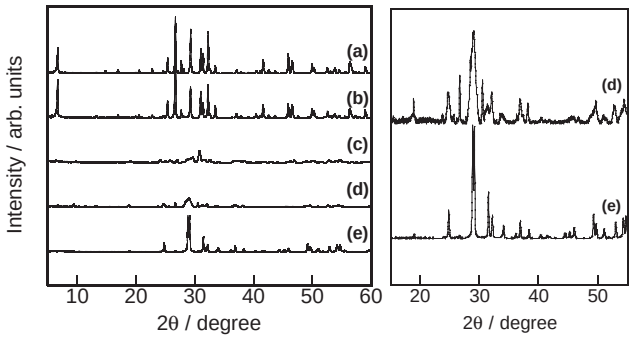

Figure 2. XRD patterns of molten $SnCl_2$-treated $Sr_2Nb_2O_7$. (a) Non-treated, (b) $Sr_2Nb_2O_7$(Sn-15 min), (c) $Sr_2Nb_2O_7$(Sn-5 h), (d) $Sr_2Nb_2O_7$(Sn-24 h), and (e) $SnNb_2O_6$(SSR).

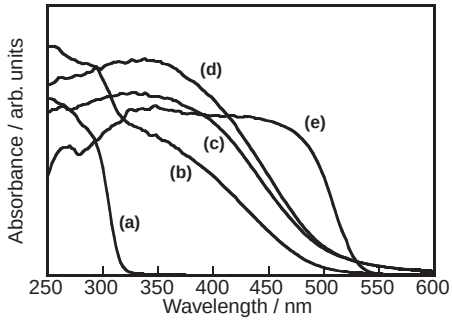

Figure 3. Diffuse reflectance spectra of $Sr_2Nb_2O_7$, $Sr_{2-x}Sn_x$-Nb_2O_7, and $SnNb_2O_6$ nanoplate. (a) Non-treated $Sr_2Nb_2O_7$, (b) $Sr_2Nb_2O_7$(Sn-15 min), (c) $Sr_2Nb_2O_7$(Sn-5 h), (d) $Sr_2Nb_2O_7$-(Sn-24 h), and (e) $SnNb_2O_6$(SSR).

In contrast, $SnNb_2O_6$(SSR) consisted of large particles (several μm) in which the primary particles (ca. 300 nm) were sintered; the surface area was 1.3 $m^2\,g^{-1}$. The synthesis temperature (573 K) of the $SnNb_2O_6$ nanoplate with the molten $SnCl_2$ treatment of $Sr_2Nb_2O_7$ was lower than that of the solid-state reaction (above 873 K). Thus, the molten $SnCl_2$ treatment is useful as a synthetic method for $SnNb_2O_6$ with a large surface area and a unique morphology.

Figure 3 shows diffuse reflectance spectra of molten $SnCl_2$-treated $Sr_2Nb_2O_7$ and $SnNb_2O_6$(SSR). It was found that the absorption edge was red-shifted and the absorption band of the visible region increased with increasing molten $SnCl_2$ treatment time. This change in the absorption band was caused by an increase in the amount of substituted Sn in $Sr_2Nb_2O_7$ at the initial stage and the amount of the $SnNb_2O_6$ phase at the late stage. The $SnNb_2O_6$ nanoplate showed a wide absorption band with an onset around 500 nm. This absorption was blue-shifted compared with that of $SnNb_2O_6$(SSR). The blue shift was also observed for Bi_2MoO_6 nanoplates.[7]

It was revealed from XRD and SEM measurements that $SnNb_2O_6$ obtained by molten $SnCl_2$-treatement of $Sr_2Nb_2O_7$ has a nanoplate shape and low crystallinity. The absorption band of this $SnNb_2O_6$ nanoplate was blue-shifted due to the quantum size effect and low crystallinity compared with that of $SnNb_2O_6$(SSR) consisted of large particle.

Table 1. Photocatalytic activities of $SnNb_2O_6$ for H_2 evolution from an aqueous methanol solution[a]

Preparation Method	Preparation Condition	SA /$m^2\,g^{-1}$	BG /eV	Activity /$\mu mol\,h^{-1}$
Solid-state reaction	1073 K-10 h	1.3	2.3	9.1[b]
Molten $SnCl_2$-treated	573 K-24 h	55.5	2.4	10.0[c]

[a]300-W Xe lamp ($\lambda > 420$ nm), Catalyst: 0.3 g, [b]0.1 g, [c]Co-catalyst: Pt 0.3 wt %, methanol solution: 150 mL.

Table 1 shows the photocatalytic activities of the $SnNb_2O_6$ nanoplate and $SnNb_2O_6$(SSR) samples under visible light irradiation. The Pt-loaded $SnNb_2O_6$ nanoplate showed photocatalytic activity for H_2 evolution from an aqueous methanol solution. This photocatalytic activity was similar to that of $SnNb_2O_6$-(SSR). Although the $SnNb_2O_6$ nanoplate had lower crystallinity and absorbance in the visible light region than $SnNb_2O_6$(SSR), their photocatalytic activities were almost the same and, moreover even under monochromatic light irradiation at 420 nm. The $SnNb_2O_6$ nanoplates did not exhibit any activity for O_2 evolution from an aqueous $AgNO_3$ solution; neither did $SnNb_2O_6$(SSR).

In conclusion, $SnNb_2O_6$ was able to be obtained by reacting $Sr_2Nb_2O_7$ with molten $SnCl_2$ at 573 K for 24 h. The $SnNb_2O_6$ consisted of nanoplates with a large surface area because it formed through breaking the layered structure of $Sr_2Nb_2O_7$. The $SnNb_2O_6$ nanoplate was active for H_2 evolution from an aqueous methanol solution under visible light irradiation ($\lambda > 420$ nm) as well as that synthesized by a solid-state reaction.

This work was supported by Core Research for Evolutional Science and Technology (CREST) of the Japan Science and Technology Agency (JST), a Grant-in-Aid (No. 14050090) for the Priority Area Research (No. 417) from MEXT, and the Nissan Science Foundation.

References

1 K. Domen, J. N. Kondo, M. Hara, T. Takata, *Bull. Chem. Soc. Jpn.* **2000**, *73*, 1307.
2 A. Kudo, H. Kato, I. Tsuji, *Chem. Lett.* **2004**, *33*, 1534.
3 J. Sato, H. Kobayashi, K. Ikarashi, N. Saito, H. Nishiyama, Y. Inoue, *J. Phys. Chem. B* **2004**, *108*, 4369.
4 H. Kato, K. Asakura, A. Kudo, *J. Am. Chem. Soc.* **2003**, *125*, 3082.
5 Y. Hosogi, K. Tanabe, H. Kato, H. Kobayashi, A. Kudo, *Chem. Lett.* **2004**, *33*, 28.
6 Y. Ebina, N. Sakai, T. Sasaki, *J. Phys. Chem. B* **2005**, *109*, 17212.
7 J. Yu, A. Kudo, *Chem. Lett.* **2005**, *34*, 1528.

Published on the web (Advance View) April 29, 2006; doi:10.1246/cl.2006.578